OPTOELECTRONICS AND ADVANCED MATERIALS – RAPID COMMUNICATIONS Vol. 1, No. 11, November 2007, p. 609 - 613

Optical properties and spectroscopic parameters of $Sm(TTA)_3(TPPO)_2$ doped PMMA

BIAO CHEN[a,b*], NING DONG[c] , JIE XU[d], HAO LIANG[b,e], YANHUA LUO[b] , CHANGMING WANG[a],
WENXUAN WU[b] , HAIGANG WANG[a]
[a]*Department of History of Science and Technology and Archaeometry,* [b] *Department of Polymer Science and Engineering, University of Science and Technology of China, Hefei 230026, China* , [c]*NingboFree Trade Zone Postdoctoral Research Station* , *Ningbo, Zhejiang 315800, P.R.China,*
[d]*Key Lab of Green Processing and Functionalisation of New Textile Materials, Ministry of Education, Wuhan University of Science & Engineering* , *Wuhan, Hubei, 430073* , *P.R.China,*
[e]*Department of Chemistry Engineering, Huizhou University, Huizhou, Guangdong 516001, PR China*

The absorption spectrum of $Sm(TTA)_3(TPPO)_2$ (TTA:thenoyltrifluoroacetone, TPPO: triphenylphosphine oxide) doped PMMA (polymethyl methacrylate) matrix at room temperature in the spectra range 400-1800 nm was measured. The energy levels are assigned and analyzed in terms of the free-ion Hamiltonian model. Energy levels and reduced matrix elements calculations are carried out using the complete 198 SLJ basis sets for the $4f^5$ configuration. Judd-Ofelt parameters have been evaluated and used to predict the radiative properties of $Sm(TTA)_3(TPPO)_2$ doped PMMA. The evaluation of the radiative properties indicates that the $^4G_{5/2}\rightarrow{}^6H_{9/2}$ transition of $Sm(TTA)_3(TPPO)_2$ doped PMMA can be considered as an efficient luminescent material.

(Received October 8, 2007; accepted October 31, 2007)

Keywords: Polymers; Radiative Properties; Rare Earth; Optical Properties, Spectroscopic Parameters, PMMA doping

1. Introduction

Rare-earth-doped inorganic glasses and crystals have been studied in detail because of their wide application in a variety of advanced materials [1-6]. Recently, rare-earth-doped polymer systems are of interest for their potential applications for laser systems, polymer optical fiber amplifier and integrated waveguides [7-12], which promote us to investigate and synthesize new rare-earth-doped polymer systems.

The design of efficient lanthanide complexes has become an important research goal, working with many different classes of ligands. In this paper, $Sm(TTA)_3(TPPO)_2$ was used for TTA was used to activate the luminescence of Sm^{3+}, and TPPO act as synergic shielding ligands, which produce antisymmetrical structures that promote faster radiation rates, because the coordination of phosphine oxide molecules can prevent coordiniation of water or solvent molecules and lower vibrations (P = O:1125 cm^{-1}) [13]. PMMA was selected as the matrix for its low optical absorption, simple synthesis and low cost. These characteristics make it suitable as a polymer matrix for rare earth ions doping. At the same time, the Sm chelates have been regarded as attractive for use as luminescent materials because of their red emission of $^4G_{5/2}\rightarrow{}^6H_{9/2}$ transition which is nearly at the low-loss windows of PMMA (650 nm). Due to these reasons, in this work, $Sm(TTA)_3(TPPO)_2$ was chosen as the dopant in PMMA.

The Judd-Ofelt theory is widely used in the theoretical analysis of optical properties of rare earth doped materials [14,15]. For the $4f^5$ ground configuration of Sm^{3+}, there are totally 198 SLJ basis states [16,17] used in the construction of the free ion Hamiltonian matrix (H matrix). It thus requires careful manipulations in the diagonalization of the H matrix to derive the energy levels and corresponding wavefunctions of Sm^{3+}, which are used in the Judd-Ofelt analysis. The high energy levels are found to be closely spaced and difficult to assign them with pure SLJ (multiplet) quantum numbers [2].

In this work, the absorption and emission spectra of $Sm(TTA)_3(TPPO)_2$ doped PMMA were measured. Using the free-ion model, parametric simulation of energy levels is performed. With the help of Judd-Ofelt theory applied, the radiative properties of $Sm(TTA)_3(TPPO)_2$ doped in PMMA are predicted.

2. Experimental section

$Sm(TTA)_3(H_2O)_2$ was prepared by the method reported before [12]. To synthesize $Sm(TTA)_3(TPPO)_2$, the chloroform doped $Sm(TTA)_3(H_2O)_2$ and TPPO was refluxed under stirring for 7 h. The molar ratio of $Sm(TTA)_3(H_2O)_2$ and TPPO is 1:2. After volatilization of the chloroform, the products were recrystallized from acetone/petroleum ether and dried under vacuum.

A solution (0.03 $mol\cdot dm^{-3}$) of $Sm(TTA)_3(TPPO)_2$ in purified MMA (methyl methacrylate) was prepared.

$Sm(TTA)_3(TPPO)_2$ doped PMMA was made by bulk polymerization. First, 30mg 2,2-Azoisobutyronitrile (AIBN) was added to the above 20 ml Sm-MMA solution and dissolved. Then the above solution was pre-polymerized at 85^o for 30 min, and the pre-polymerized solution was poured into a model. The polymerization of the model was carried out at 50^o for 24 h and additionally heated at 90℃ until solidification was fulfilled. The sample was cut and polished for optical measurements.

The absorption spectra from 400 to 1800 nm were recorded with a Perkin-Elmer model Lambda 900 spectrometer at room temperature. The emission spectrum was analyzed with a 44W monochromator equipped with a Hamamatsu R456 photomultiplier.

3. Results and discussion

3.1. Absorption spectrum

Fig. 1 shows the absorption spectrum of $Sm(TTA)_3(TPPO)_2$ doped PMMA in the wavelength range 400–1800 nm at room temperature, and the inset is the enlargement of $^6H_{5/2} \rightarrow {}^4I_{13/2}$, $^4I_{11/2}$, $^4I_{9/2}$, $^4F_{3/2}$. All the absorption bands are attributed to the excitation from the ground state, $^6H_{5/2}$, to various excited states and the assignments of the bands are given in the figure.

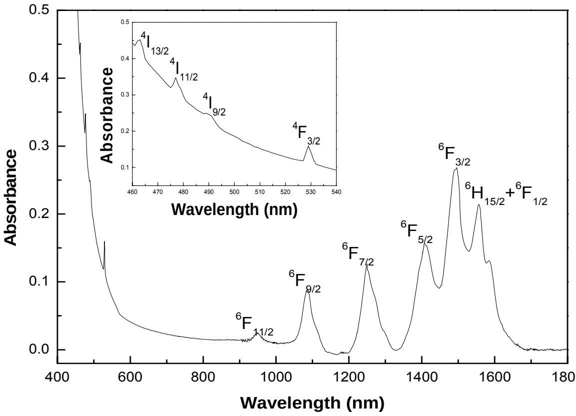

Fig. 1 Absorption spectrum of $Sm(TTA)_3(TPPO)_2$ *doped PMMA The inset is the enlargement of* $^6H_{5/2} \rightarrow {}^4I_{13/2}$, $^4I_{11/2}$, $^4I_{9/2}$, $^4F_{3/2}$.

3.2. Simulation of the free ion energy level scheme

For the $4f^5$ configuration of Sm^{3+}, the free-ion energy levels can be derived by diagonalizing the free-ion Hamiltonian between the 198 (complete) SLJ basis states. The free-ion Hamiltonian of Sm^{3+} may be expressed explicitly as follows [17]:

$$H_{FI} = E_{AVG} + \sum_{k=2,4,6} F^k f_k + \zeta_{SO} A_{SO} + \alpha L(L+1) + \beta G(G_2) + \gamma G(R_7) + \sum_{i=2,3,4,6,7,8} T^i t_i + \sum_{k=2,4,6} P^k p_k + \sum_{j=0,2,4} M^j m_j \qquad (1)$$

Here E_{AVG} represents the spherically symmetric part of the free-ion Hamiltonian; the rest parameters (Slater parameters F^k; spin-orbit interaction ζ; wo-body correction α, β, γ ; three-body correction T^i; electrostatic correlated spin-orbit P^k and Marvin's integrals M^j) and their associated operators are induced corresponding to the interactions they represent. The operators represent angular integrals and their associated parameters represent radial integrals [2].

Table 1 . Experimental and calculated values for the energies (cm^{-1}) *of* $Sm(TTA)_3(TPPO)_2$.

SLJ	S′L′J′	E_{exp} (cm^{-1})	E_{cal} (cm^{-1})
$^6H_{5/2}$	$^6H_{5/2}$	0	4.49
	$^6H_{7/2}$	--	1034.23
	$^6H_{9/2}$	--	2235.91
	$^6H_{11/2}$	--	3557.19
	$^6H_{13/2}$	--	4957.30
	$^6F_{1/2}$	6309.15	6382.79
	$^6H_{15/2}$	6422.61	6401.88
	$^6F_{3/2}$	6684.49	6630.32
	$^6F_{5/2}$	7107.32	7127.41
	$^6F_{7/2}$	7993.61	7984.99
	$^6F_{9/2}$	9208.10	9154.30
	$^6F_{11/2}$	10504.20	10540.92
	$^4G_{5/2}$	17863.00	17830.75
	$^4F_{3/2}$	18903.59	18907.37
	$^4G_{7/2}$	--	19961.93
	$^4I_{9/2}$	20408.16	20467.68
	$^4M_{15/2}$	--	20740.64
	$^4I_{11/2}$	20964.36	21003.00
	$^4I_{13/2}$	21598.27	21529.09

The free ion parameters shown in Table 2 are obtained by a least square fitting procedure between the observed and calculated energy levels. The mean square deviation σ is employed to evaluate the fitting results, which is expressed as follows:

$$\sigma = \sqrt{\sum (E_{\exp} - E_{cal})^2 / (p-q)} \tag{2}$$

where E_{exp} and E_{cal} are the observed and calculated energy levels, with p and q correspond to the number of experimental energy levels and the number of variable parameters used in the fitting process. In our calculation, the values of the parameters T^i, P^k and M^j, are held fixed with values from the literature [18], while those of the parameters E_{AVG}, F^k, ζ, α, β and γ are varied freely with the initial values from the literature [18]. The number of parameters used as fitting variables depends on the quality and quantity of the experimental data and on the types of levels represented in the respective data sets. The experimental and calculated energy levels of $Sm(TTA)_3(TPPO)_2$ doped PMMA are given in Table 1 and the parameters used in the free-ion simulation are listed in Table 2.

The final mean square deviation σ in our calculation results to be 59.04 cm^{-1}, which represents a quite good fitting process [18].

Table 2 . Free-ion parameters for $Sm(TTA)_3(TPPO)_2$.

Parameters	Values (cm^{-1})
E_{AVG}	47478.46
F^2	78992.13
F^4	57298.96
F^6	39117.33
α	21.50
β	-813.32
γ	1916.00
ζ	1164.07
σ	59.04

The following parameter values were held fixed in performing the data fits (in the unit of cm^{-1}) [19]: $T^2 = 283$, $T^3 = 30$, $T^4 = 100$, $T^6 = -231$, $T^7 = 265$, $T^8 = 319$, $M^0 = 2.34$, $P^2 = 315$.

3.3. Judd-Ofelt analysis

A prerequisite for the intensity calculation is the computation of complete intermediate coupling eigenvectors for the energy levels investigated [20]. Based on the free-ion Hamiltonian model presented in Sec. 3.2, all the squared reduced matrix elements were obtained and listed in Table 3.

Table 3. Values of the energies and squared reduced matrix elements of $Sm(TTA)_3(TPPO)_2$ doped PMMA..

SLJ	S′L′J′	υ(cm^{-1})	$\|\|U^2\|\|^2$	$\|\|U^4\|\|^2$	$\|\|U^6\|\|^2$
$^6H_{5/2}$	$^6H_{7/2}$	1034.23	0.2057	0.1979	0.0935
	$^6H_{9/2}$	2235.91	0.0257	0.1401	0.3249
	$^6H_{11/2}$	3557.19	0	0.024	0.2649
	$^6H_{13/2}$	4957.30	0	0.0007	0.0662
	$^6F_{1/2}$	6382.79	0.1947	0	0
	$^6H_{15/2}$	6401.88	0	0	0.0043
	$^6F_{3/2}$	6630.32	0.1313	0.1293	0
	$^6F_{5/2}$	7127.41	0.0268	0.2543	0
	$^6F_{7/2}$	7984.99	0.0015	0.1258	0.3907
	$^6F_{9/2}$	9154.30	0	0.0187	0.3167
	$^6F_{11/2}$	10540.92	0	0.0006	0.0516
	$^4G_{5/2}$	17830.75	0.0046	0.0028	0
	$^4F_{3/2}$	18907.37	0.0135	0.0052	0
	$^4G_{7/2}$	19961.93	0.0014	0.0002	0.0162
	$^4I_{9/2}$	20467.68	0.0026	0.0006	0.0015
	$^4M_{15/2}$	20740.64	0	0	0.0334
	$^4I_{11/2}$	21003.00	0	0	0.0112
	$^4I_{13/2}$	21529.09	0	0.0031	0.0236
$^4G_{5/2}$	$^6H_{5/2}$	17826	0.0046	0.0028	0
	$^6H_{7/2}$	16796	0.0023	0.0097	0.023
	$^6H_{9/2}$	15595	0.0059	0.025	0.0016
	$^6H_{11/2}$	14273	0	0.006	0.0023
	$^6H_{13/2}$	12873	0	0.0042	0.0116
	$^6H_{15/2}$	11448	0.0012	0	0
	$^6F_{1/2}$	11429	0	0	0.0075
	$^6F_{3/2}$	11200	0.0006	0.0001	0
	$^6F_{5/2}$	10703	0.0028	0.0003	0
	$^6F_{7/2}$	9846	0.0025	0.0015	0
	$^6F_{9/2}$	8676	0.0044	0.0009	0
	$^6F_{11/2}$	7290	0	0.0002	0.0025

The oscillator strength of an absorption band is determined experimentally using the following equation [18]:

$$P_{\exp} = 4.318 \times 10^{-9} \int \varepsilon(\nu) d\nu \tag{3}$$

where $\varepsilon(\nu)$ is the molar extinction coefficient (per molar concentration per centimeter) at the energy ν (cm^{-1}) which has been evaluated from Beer's law.

According to the Judd-Ofelt theory [14,15], the oscillator strengths between the initial J and final J′ multiplet are giving by [20] :

$$P_{JJ'} = \frac{8\pi^2 mc\chi\nu}{3h(2J+1)} \times \sum_{\lambda=2,4,6} \Omega_\lambda \times \left\langle f^N[\gamma,S,L]J \left\| U^{(\lambda)} \right\| f^N[\gamma',S',L']J' \right\rangle^2 \tag{4}$$

where m is the mass of electron, c is the velocity of light, h is the Plank constant, $\chi = \frac{(n^2+2)^2}{9n}$ is the local field correction factor, $n=1.495$ is the refractive index, ν is the frequency in inverse centimeters. The $f^N[\gamma,S,L]$ are wave functions which are obtained from the free ion energy level calculations described in Sec.3.2. These wave functions are linear combinations of the basis SLJ wave functions of $4f^2$ configuration.

Using the oscillator strengths, the Judd-Ofelt parameters Ω_λ can be obtained by a least-square method. And the *rms* deviation is calculated in the usual way.

The experimental and calculated oscillator strengths for the absorption bands, Judd-Ofelt parameters and rms deviations of $Sm(TTA)_3(TPPO)_2$ doped PMMA are listed in Table 4.

From Table 4, the *rms* deviation is $\pm 0.41\times10^{-6}$ for $Sm(TTA)_3(TPPO)_2$ doped PMMA and is comparable with previous studies of other samarium systems [2,3].

Table 4 . Experimental and calculated oscillator strengths and Judd-Ofelt parameters of $Sm(TTA)_3(TPPO)_2$ doped PMMA

$(S',L')J'$	P_{exp} (10^{-6})	P_{calc} (10^{-6})
$^6F_{1/2}+^6H_{15/2}+^6F_{3/2}$	19.66	19.66
$^6F_{5/2}$	6.32	6.32
$^6F_{7/2}$	8.14	8.13
$^6F_{9/2}$	5.47	5.41
$^6F_{11/2}$	0.74	0.87
$^4F_{3/2}$	0.60	0.04
$^4I_{9/2}$	0.38	0.42
$^4M_{15/2}+^4I_{11/2}$	0.64	1.38
$^4I_{13/2}$	0.61	0.93
$\Omega_2\times10^{-20}cm^2$	32.92	
$\Omega_4\times10^{-20}cm^2$	11.09	
$\Omega_6\times 10^{-20}cm^2$	7.06	
$\delta_{rms}\times10^{-6}$	0.41	

3.4. Radiative properties

Fig. 2 shows the fluorescence spectrum of $Sm(TTA)_3(TPPO)_2$ doped PMMA from 500 to 700 nm. The fluorescence spectrum was obtained by excitation at the 476.5 nm Ar line.

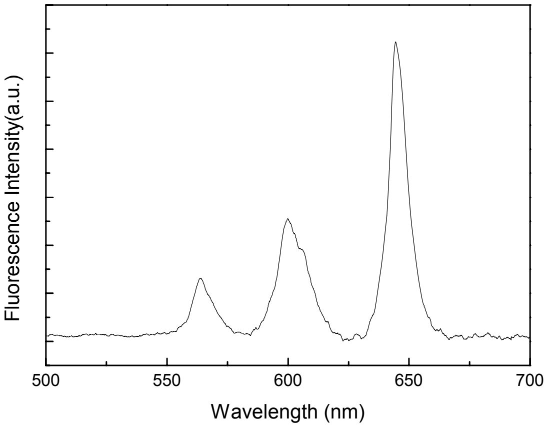

Fig. 2. Fluorescence spectrum of $Sm(TTA)_3(TPPO)_2$ under 476.5 nm excitation.

From the Judd-Ofelt parameters Ω_λ obtained above, the radiative transition lifetime τ_R of $^4G_{5/2}$ level is determined to be 0.808 ms. The radiative lifetime of the transition involved is an important parameter in consideration of the pumping requirement for the threshold of laser action and the calculated radiative lifetime is about 0.808 ms. It is comparable with the radiative lifetimes of samarium laser glasses[21].

Using the Judd-Ofelt parameters Ω_λ and fluorescence spectrum of $Sm(TTA)_3(TPPO)_2$ doped PMMA, the emission cross sections of $^4G_{5/2}\rightarrow^6H_J$ (J=9/2,7/2,5/2) are calculated and the results are listed in Table 5. The emission cross section σ_p is one of the most important parameters for luminescent material. The emission cross section σ_p of $^4G_{5/2}\rightarrow^6H_{9/2}$ fluorescence transition of $Sm(TTA)_3(TPPO)_2$ doped PMMA is 6.25×10^{-21} cm^2, which is comparable with those shown by glasses used in the solid state laser applications[3,21].

Table 5 . Predicted optical properties and emission cross section of $Sm(TTA)_3(TPPO)_2$ doped PMMA.

Transition	λ(nm)	$\sigma(cm^2)$
$^4G_{5/2}\rightarrow^6H_{9/2}$	645	6.25×10^{-21}
$^4G_{5/2}\rightarrow^6H_{7/2}$	601	1.18×10^{-21}
$^4G_{5/2}\rightarrow^6H_{5/2}$	564	5.37×10^{-22}

4. Conclusions

A detailed study on the optical properties of $Sm(TTA)_3(TPPO)_2$ doped PMMA has been carried out. The absorption spectrum of $Sm(TTA)_3(TPPO)_2$ doped PMMA is analyzed. With the free-ion Hamiltonian model, all the energy levels are assigned and the reduced matrix elements are calculated. The evaluation of the radiative properties indicates that the $^4G_{5/2}\rightarrow^6H_{9/2}$ transition of $Sm(TTA)_3(TPPO)_2$ doped PMMA can be considered as an efficient luminescent material.

Acknowledgements

This work was supported by China Postdoctoral Science Foundation (No: 20060400733) and the National Natural Science Foundation of China (No: 50573071). The authors gratefully acknowledge the financial support and wish to express their thanks to the referees for critically reviewing the manuscript and making important suggestions.

References

[1] W. F. Krupke, Phys. Rev. **145**(1), 325 (1966).
[2] C. K. Jayasankar, P. Babu, J. Alloy. Compd. **307**, 82 (2000).

[3] A. Kumar, D. K. Rai, S. B. Rai, Spectrosc. Acta A – Molec. Biomolec. Spectr. **59**, 917 (2003).
[4] J. Zhu, Mater. Lett. **59**, 1413 (2005).
[5] B. Eraiah, S. G. Bhat, J. Phys. Chem. Solids **68**, 581 (2007).
[6] U. P. Singh, R. Kumar, S. Upreti, J. Mol. Struct. **831**, 97 (2007).
[7] C. Koeppen, S. Yamada, G. Jiang, A. F. Garito, J. Opt. Soc. Am. B **14**, 155 (1997).
[8] K. Kuriki, S. Nishihara, Y. Nishizavva, A. Tagaya, Y. Okamoto, Y. Koike, Electron. Lett. **37**, 415 (2001).
[9] K. Kuriki, Y. Koike, Chem. Rev. **102**, 2347 (2002).
[10] B. Chen, N. Dong, J. Xu, H. Liang, Q. J. Zhang, M. Yin，Spectroc. Acta Pt. A-Molec. Biomolec. Spectr. **63**, 289 (2006).
[11] Q. Meng, P. Boutinaud, H. Zhang, Rachid Mahiou, J. Lumin. **124**, 15 (2007).
[12] M. Iwamuro, Y. Hasegawa, Y. wada, K. Murakoshi, N. Nakashima, T. Yamanaka, S. Yanagida, J. Lumin. **79**, 29 (1998).
[13] Y. Hasegawa, M.I Yamamuro, Y. Wada, N. Kanehisa, Y. Kai, S. Yanagida, J. Phys. Chem. A **107**, 1697 (2003).
[14] B. R. Judd, Phys. Rev. **127**, 750 (1962).
[15] G. S. Ofelt, J. Chem. Phys. **37**, 511 (1962).
[16] P. S. May, M.F. Reid, F.S. Richardson, Mol. Phys. **61**, 1455 (1987).
[17] C. Gorller-Walrand, K. Binnemans, Spectral intensities of f-f transitions, in: Gschneidner KA Jr., Eyring L (Eds.), Handbook on the Physics and Chemistry of Rare Earths, Vol. 23, Amsterdam: Elsevier, 1996.
[18] W. T. Carnall, P. R. Fields, K. Rajnak, J. Chem. Phys. **49**, 4412 (1968).
[19] R. P. Leavitt, J. B. Gruber, N. C. Chang, C. A. Morrison, J. Chem. Phys. **76**, 4775 (1982).
[20] W. T. Carnall, P. R. Fields, B. G. Wybourne, J. Chem. Phys. **42** 3797 (1965).
[21] M. C. Farries, P. R. Morkel, J. E. Townsend, Electron. Lett. **24**, 709 (1988).

---

[*] Corresponding author: chenbiao@ustc.edu.cn